Microbial Ecology (2020) 80:286–295
https://doi.org/10.1007/s00248-020-01493-x

ENVIRONMENTAL MICROBIOLOGY

Meta-omics Provides Insights into the Impact of Hydrocarbon Contamination on Microbial Mat Functioning

Johanne Aubé[1,2] · Pavel Senin[1,3] · Patricia Bonin[4] · Olivier Pringault[5] · Céline Jeziorski[6] · Olivier Bouchez[6] · Christophe Klopp[3] · Rémy Guyoneaud[1] · Marisol Goñi-Urriza[1]

Received: 23 November 2018 / Accepted: 4 February 2020 / Published online: 19 February 2020

Abstract

Photosynthetic microbial mats are stable, self-supported communities. Due to their coastal localization, these mats are frequently exposed to hydrocarbon contamination and are able to grow on it. To decipher how this contamination disturbs the functioning of microbial mats, we compared two mats: a contaminated mat exposed to chronic petroleum contamination and a reference mat. The taxonomic and metabolic structures of the mats in spring and fall were determined using metagenomic and metatranscriptomic approaches. Extremely high contamination disturbed the seasonal variations of the mat. ABC transporters, two-component systems, and type IV secretion system-related genes were overabundant in the contaminated mats. Xenobiotic degradation metabolism was minor in the metagenomes of both mats, and only the expression of genes involved in polycyclic aromatic hydrocarbon degradation was higher in the contaminated mat. Interestingly, the expression rates of genes involved in hydrocarbon activation decreased during the 1-year study period, concomitant with the decrease in easily degradable hydrocarbons, suggesting a transient effect of hydrocarbon contamination. *Alteromonadales* and *Oceanospirillales* hydrocarbonoclastic bacteria appeared to be key in hydrocarbon remediation in the contaminated mat. Overall, the contaminated microbial mat was able to cope with hydrocarbon contamination and displayed an adaptive functioning that modified seasonal behaviour.

Keywords Microbial mats · Metabolism · Metagenomics · Metatranscriptomic · Functioning · Diversity

Introduction

Photosynthetic microbial mats growing in coastal areas are among the most diverse and complex marine ecosystems [1]. The overall metabolism of a microbial mat is driven by solar light as the main energy source. Microbial activities generate physical and chemical gradients in the mat that maintain the structure and activity of the mat's community [2], leading to a stable, self-supported mat. Microbial mats are highly dynamic and are subjected to strong fluctuations at the diel or seasonal scales [2]. The extensive genetic and metabolic diversity of photosynthetic microbial mat-inhabiting organisms enables development in a wide variety of environments, including hot springs, hypersaline and alkaline environments and polar ponds [1, 3–6]. Due to their localization in coastal zones, microbial mats are frequently subjected to hydrocarbon contamination [7, 8]. The response of microbial mats to petroleum contamination has been studied in microcosm experiments and under natural conditions after acute pollution events (accidental or laboratory experiments). Microbial mats can cope with contamination and develop a robust community

Electronic supplementary material The online version of this article (https://doi.org/10.1007/s00248-020-01493-x) contains supplementary material, which is available to authorized users.

✉ Marisol Goñi-Urriza
marisol.goni@univ-pau.fr

[1] Environmental Microbiology, Universite de Pau et des Pays de l'Adour, E2S UPPA, CNRS, IPREM, Pau, France

[2] Present address: Laboratoire de Microbiologie des Environnements Extrêmes, UMR6197, IFREMER, CNRS, Université de Bretagne Occidentale, Plouzané, France

[3] Plateforme Bioinformatique Genotoul, UR875 Biométrie et Intelligence Artificielle, INRA, Castanet-Tolosan, France

[4] Mediterranean Institute of Oceanography (MIO), Aix Marseille University, Université de Toulon, CNRS/INSU/IRD, UM 110, Marseille, France

[5] UMR 9190 MARBEC IRD-Ifremer-CNRS, Université de Montpellier, Place Eugène Bataillon, Montpellier, France

[6] GeT-PlaGe, Genotoul, INRA Auzeville, Castanet-Tolosan, France

adapted to petroleum levels [8, 9]. The few studies that have focused on chronic oil pollution have concluded that the structure of microbial mats is related to the level of contamination [8] and that contaminated mats can degrade hydrocarbons [10, 12]. Generally, noticeable changes in composition [8, 10] of high contaminated mats are reported, and some studies described lower diversity in higher contaminated mats [13], but not overabundance of hydrocarbonoclastic microorganisms have been observed. Nevertheless, when these contaminated mats were submitted to fresh oil pollutions, an immediate induction of RHD genes involved in polyaromatic hydrocarbon degradation was observed, accompanied with an efficient degradation of crude oil [10]. This metabolic response (associated with a community structural shift [12]) was however quickly reversed, highlighting a fast, adaptive and efficient response of the metabolically active bacterial population. Oil contamination also impacts typical seasonal behaviour of photosynthetic microbial mats, by strongly inhibiting primary production and respiration in spring, but with no significant impact in fall [20]. As consequences, the typical overabundance of *Cyanobacteria* in fall compared with spring could not be observed in the higher contaminated mat [19]. These studies were performed using taxonomic and/or metabolic gene markers, such as ribosomal genes or genes involved in hydrocarbon degradation [9–14].

High-throughput sequencing of metagenomes and metatranscriptomes has provided an unprecedented overview of the functional capacities and gene expression of microbial communities confronting environmental stresses. As the presence and expression of genes involved in hydrocarbon degradation (including complete metabolic pathways) have been observed in oil spill-contaminated seawaters [15–17] and soils [18, 19], applying these sequencing techniques to contaminated microbial mats will provide new insights on the adaptation of microbial mats to hydrocarbon contamination.

The aim of this paper was to elucidate the impact of long-term petroleum contamination on the functioning of microbial mats. Two photosynthetic microbial mats located in the Berre lagoon, a brackish lagoon bordering the Mediterranean Sea in the South of France, were investigated in this work. These mats feature similar physical and chemical parameters (salinity, temperature, solar irradiation, etc.) [20] but have been subjected to differing hydrocarbon contamination levels. Specifically, the contaminated mat received hydrocarbon inputs from a petrochemical industry site for more than 80 years. By applying metagenome and enriched mRNA metatranscriptome sequencing, we described the key metabolic pathways of both microbial mats. Comparing the contaminated mat with the reference mat revealed the role of petroleum pollution in microbial community functioning. A deeper analysis of metabolism related to hydrocarbon degradation pathways was also performed.

Material and Methods

Sampling Sites and Procedure

Berre lagoon is located on the Mediterranean French coast. Microbial mat samples were collected from two sites in the lagoon: a reference station located in the bird reserve "Les salins du Lion" (SL) (43.452570 N 5.230085 E) and a contaminated station located in a retention basin receiving hydrocarbon-contaminated rainfall water from a petrochemical industry site (EDB1) (43.484946 N 5.188452 E) [8, 21]. At this latter site, the hydrocarbon content reaches 96 μg/g [8]. In addition to this chronic contamination, an accidental oil spill occurred in September 2009 due to the overflow of a hydrocarbon-polluted water retention pond [22], which increased the hydrocarbon content. Three sampling exercises were performed: one in spring (April 2012) and two in fall (September 2011 and 2012), which were named Apr12, Sept11 and Sept12, respectively. A piece of mat (around 1.5 m^2), including the top 2 cm of sediment, was collected at mid-day as described in [19]. Subsamples for molecular analyses were stored at − 80 °C. A description of main physical-chemical characteristics and hydrocarbon composition of both sites can be found at Table S1.

Whole Metagenome and Metatranscriptome Sequencing and Bioinformatic Procedures

DNA and RNA were co-extracted in triplicate using an RNA PowerSoil Total RNA Isolation Kit (MO BIO Laboratories, Inc.) coupled with an AllPrep DNA/RNA Mini Kit (QIAGEN) for DNA and RNA separation. RNA was digested with an RNase-Free DNase Set (QIAGEN) for DNA removal, and RNA quality was checked as described by Aubé and coworkers [20]. Genomic DNA libraries were constructed using a NEXTflex PCR-Free DNA Sequencing Kit from BioScientific PCR-free kit following the manufacturer's protocol. RNA-seq libraries were prepared according to Illumina's protocol on a Tecan EVO200 liquid handler. An Illumina TruSeq Stranded mRNA sample prep kit was used to analyse RNA after mRNA enrichment using an Epicentre Ribo-Zero rRNA removal kit. RNA was fragmented to generate double-stranded cDNA. Ten cycles of PCR were used to amplify libraries following manufacturer's instructions (Illumina TruSeq Stranded mRNA library prep kit, Cat. No. RS-122-2101), and the libraries were precisely quantified by qPCR using a KAPA Library Quantification Kit. RNA-seq and gDNA sequencing were performed with an Illumina HiSeq2500 instrument using a paired-end read length of 2 × 100 bp with an Illumina TruSeq SBS sequencing kit v3.

The Trim Galore! utility was used for read quality control http://www.bioinformatics.babraham.ac.uk/projects/trim_galore/). Possible adapter sequences based on the Illumina

TruSeq Adapter index were removed from the reads. Data filtering was performed with cutadapt [23] and FASTX-Toolkit (http://hannonlab.cshl.edu/fastx_toolkit/index.html) by trimming reads with a Q score of less than 15 at the 3′ end, trimming unidentified dNTP (N) at the read ends and discarding reads with Ns > 10%. Reads shorter than 50 bp with low-quality bases (Q < 20) were also discarded. For functional and taxonomic annotations, all filtered reads (DNA and mRNA) were aligned to the KEGG gene database [24] using LAST aligner v392 [25]. Each read was then annotated using the single-directional best hit information method [26] with an identity cut-off of 60% and a score of 96. Eukaryotic sequences were removed from the dataset. Statistics of the reads at each bioinformatic analysis step are shown in the supplementary material (Table S2).

Statistical Analysis

Before statistical analysis, random sampling of filtered data was performed to obtain the same number of reads per sample (i.e. the minimum number of sequences in metagenomic or metatranscriptomic samples (Table S2)) and the means of the pseudo-triplicates were calculated to perform statistical tests. Taxonomic biomarkers of hydrocarbon contamination were detected using the LEfSe algorithm [27]. The first analysis step was a non-parametric Kruskal-Wallis (KW) sum-rank test to detect taxa and functional pathways with significant differential abundances. Biological consistency was subsequently investigated using a pairwise Wilcoxon test. Finally, linear discriminant analysis (LDA) was used to estimate the effect size of each differentially abundant taxon. Alpha values of 0.05 were used for the KW and Wilcoxon tests, and a threshold of 2 was used for the logarithmic LDA scores. Gene and transcript abundances for functional data were compared using a two-group White's non-parametric t test in STAMP [28] by KEGG subsystem. To account for the variation of transcriptional activity, the gene expression rate was calculated as described by Stewart et al. [29]. Hydrocarbon content was analysed by principal component analysis (PCA) using the FactoMineR package [30]; variables with cos2 below 0.5 on each factorial plane are not shown on the corresponding correlation circles of the PCA.

Accession Number

The sequence data are available in the Sequence Read Archive of the National Center for Biotechnology Information under accession number SRP063590.

Results and Discussion

Microbial mats are highly stratified systems, in which microorganisms' metabolism supports their physical and chemical structure. In return, physical and chemical conditions of the mats favour microbial specific metabolisms: structure and function are thus slightly dependent. The goal of the present study was to determine if pollution changes metabolic profiles and its consequences on coastal mat's structure and functioning.

Structure of Microbial Mat Communities

The metagenomes and metatranscriptomes of the microbial mats were annotated using the KEGG database. Between 24.70% and 46.86% of the metagenome and metatranscriptome sequences, respectively, aligned to the KEGG database (Table S2). The community composition based on the taxonomic affiliations of protein-encoding genes revealed a structure similar to that described by 16S rRNA gene affiliations [20] and to those of other mats [31, 32]; i.e. *Proteobacteria*, *Cyanobacteria* and *Bacteroidetes* were dominant (Fig. 1) with metagenomes' mean relative abundance of 48.1%, 16.0% and 15.5%, respectively. The high similarity between the structure described here and those described in previous studies on the same mats based on 16S rDNA sequences [8, 19] supported the robustness of the annotation approach. *Oscillatoriales* dominated among *Cyanobacteria*. The relative abundance of *Cyanobacteria* was highest in the EDB1 Sept12 metagenomes and metatranscriptomes, with a greater abundance of *Rivulariaceae* (Table S3). Among the *Deltaproteobacteria* (10.8% of the metagenomes' mean relative abundance), most of the sequences were affiliated with sulphate reducers in the order *Desulfobacterales* (Table S3). The sequences related to *Gammaproteobacteria* (15.0% of the metagenomes' mean relative abundance) were affiliated with *Alteromonadales* and *Chromatiales*; most of the *Chromatiales* were purple sulphur bacteria. Among the *Alpha* and *Betaproteobacteria* (17.1% and 4.3% of the metagenomes' mean relative abundance), *Rhodobacterales* and *Burkholderiales* dominated, respectively. Consistent with observations in the Guerrero Negro hypersaline microbial mats and Highborne Cay mat (The Bahamas) [33, 34], *Archaea* were in the minority in the microbial communities, accounting for 1 to 3% of total reads and mainly represented by the methanogens *Methanomicrobia*. Thus, both mats are classical mats with dominance of photosynthetic bacteria and bacteria involved in the sulphur cycle (sulphate reducers and sulphur oxidizers [2]).

The community structures described using metatranscriptomic data differed from those described by metagenomic data (Fig. 1). Remarkably, transcripts related to *Cyanobacteria* highly dominated the communities in both mats, accounting for 36.5 to 78% of the reads, highlighting the major role of *Cyanobacteria* compared with other functional groups in the mats [34, 35].

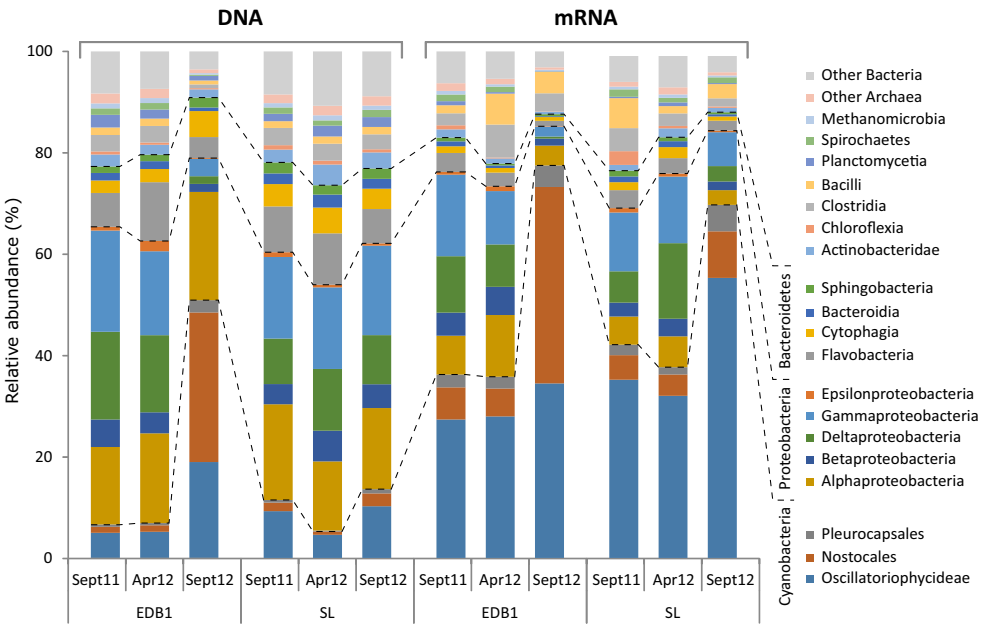

Fig. 1 Metagenome (DNA based) and metatranscriptome (mRNA based) taxonomic structure at the class level based on the affiliation of sequences. The figure shows the fraction of reads that hits with the KEGG database. Data represent the mean of triplicates. EDB1: highly contaminated mat; SL: reference mat. The dashed lines separate from the bottom to the top: *Cyanobacteria*, *Proteobacteria* and *Bacteroidetes*

As microbial mat functioning is dependent on the seasonal period [36], sampling was performed in spring and fall to assess the seasonal variation of the structure and activity of the mats. The reference mat showed typical seasonal variations characterized by (1) an increase of *Cyanobacteria* in fall (around 13% of metagenomic data in spring and 19% in fall, Table S3) and (2) an increase of the sulphur-related microorganisms in spring. This increase was observed either at metagenomic (from near 14% in fall to 19% in spring) or at metatranscriptomic level (a mean of 6% in fall and 21% in spring, Table S3) and mainly concerned *Desulfobacterales* and *Chromatiales*. On the contrary, no seasonal variations were observed in the contaminated mat: *Cyanobacteria* highly dominated the community in Sept12 but not in Sept11 samples, and a continuous decrease of the relative abundance of microorganisms related to sulphur cycle, either at metagenomic or metatranscriptomic level, was observed in the contaminated mat (Table S3).

Metabolism of Microbial Mat Communities

A total of 7009 different KEGG ortholog groups (KOs) were detected in the metagenome, and 6470 KOs were detected in the metatranscriptome. Among the annotated reads, around 44% of the microbial mat metagenomes matched genes involved in pathways associated with metabolism (Fig. 2), including 10.2–11.1% related to genes involved in carbohydrate metabolism (547 KOs) and 9.9–10.8% related to amino acid

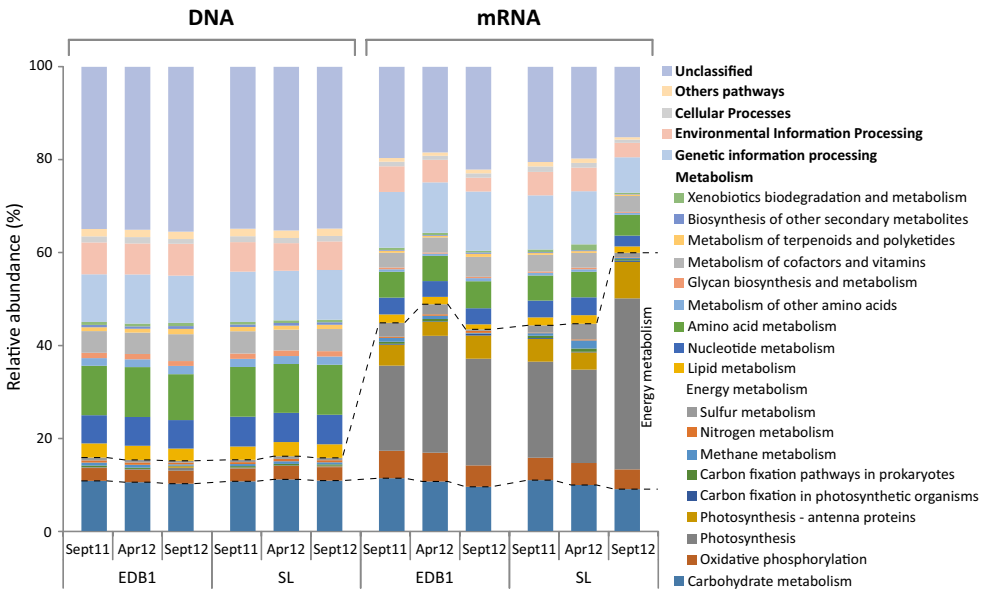

Fig. 2 Metabolic structure of the metagenome and metatranscriptome of both microbial mats based on KO assignation and pathways of sequences (relative abundance). Data represent the mean of triplicates. EDB1: highly contaminated mat; SL: reference mat. The dashed lines separate the energy metabolic pathways

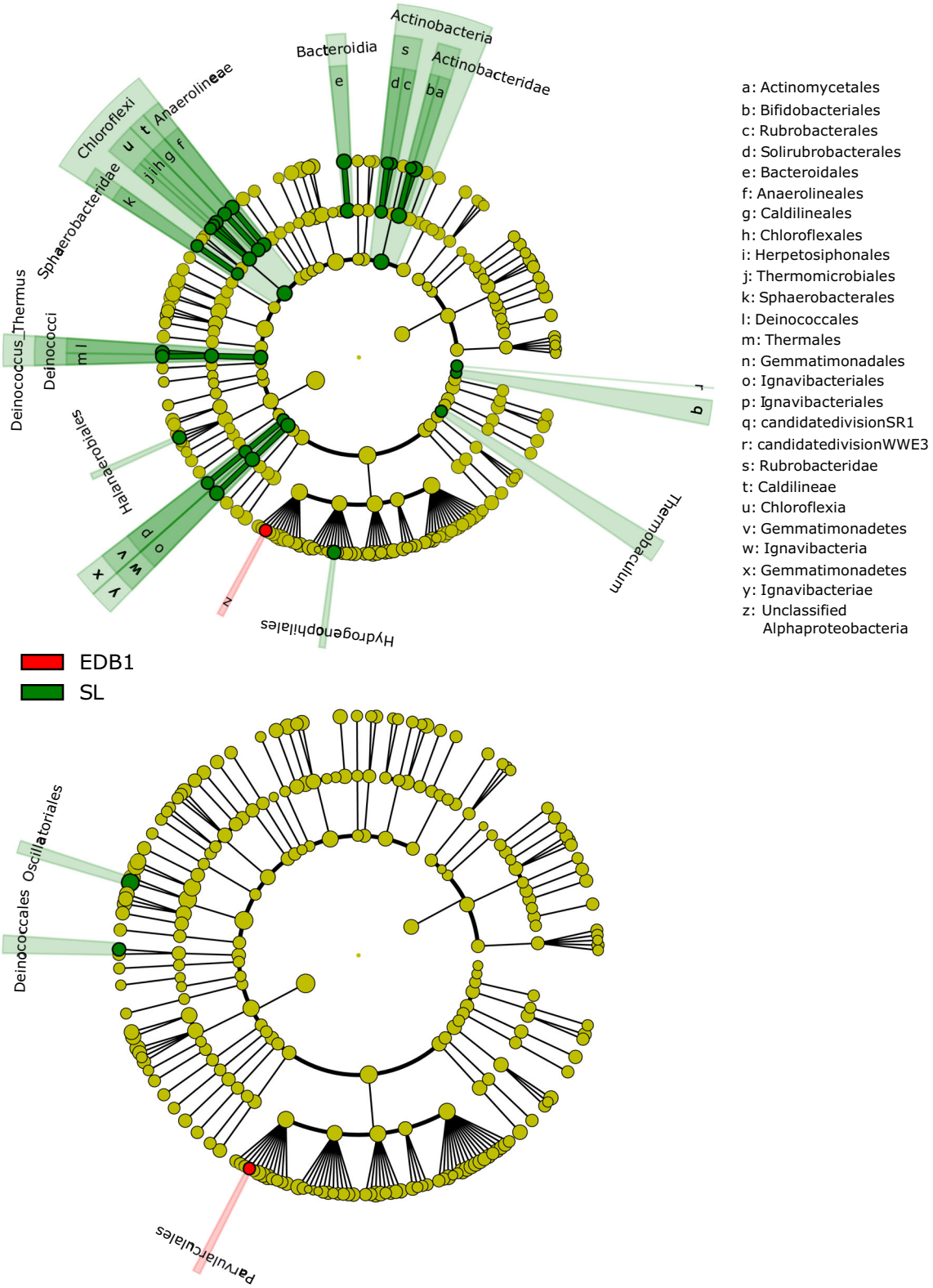

Fig. 3 LEfSe analysis of the microorganisms differentially abundant (metagenomes; **a**) and active (metatranscriptomes; **b**) in contaminated (EDB1, red) and reference (SL, green) microbial mats. Roots of cladograms stand for the domain, and concentric circles represent the following taxonomic levels until the order. Only class with *p* value below 0.05 are shown

metabolism (420 KOs). Energy metabolism–related sequences represented only 4.1–4.5% of the metagenomes but up to 49.9% of the metatranscriptomes (389 and 381 KOs for genes and transcripts, respectively). Among them,

photosynthesis metabolism–related genes (i.e. genes encoding proteins of photosystems I and II (P700 and P680) and phycobiliproteins (phycocyanin, allophycocyanin and phycoerythrin subunits)) exhibited maximum expression rates of 1094. Genes related to nitrogen and sulphur metabolism exhibited high expression rates as well. Sequences related to nitrogen metabolism were mainly involved in nitrogen fixation (i.e. nitrogenase enzyme complex); among them, *nifH* exhibited expression rates as high as 5.85. The sequences related to the sulphur cycle were involved in sulphate reduction: adenylyl-sulphate reductase and sulphite reductase (AprAB and DsrAB) exhibited maximum expression rates of 8.83 (data not shown).

While reference mat showed a typical seasonal behaviour, contaminated mat did not show the same behaviour. In this case, the comparison of metabolic potentials of both mats in order to define which of them are related to the contamination is challenging. For further analysis on hydrocarbon contamination impact on microbial mat functioning, all the samples for each mat (reference or contaminated) have been averaged. This approach could probably dissimulate some metabolisms, but eliminates the errors originating from a seasonal divergent functioning.

Metabolic and Taxonomic Differences Between Sites with Focus on Metabolic Pathways Associated with Xenobiotic Degradation

Microbial communities from coastal environments impacted by punctual oil input have been intensively studied (e.g. [16, 37, 38]), and a decrease in microbial diversity associated with dominance of hydrocarbon-degrading marine bacteria is generally observed following an oil spill [39]. By contrast, in this study, dominance of hydrocarbonoclastic bacteria in the contaminated mat compared with the reference mat was not observed, consistent with previous studies of chronically contaminated sites [8, 40]. At the taxonomic level, 36 and 3 differentially abundant taxa were detected based on metagenomic and metatranscriptomic data, respectively (Fig. 3). At the metagenomic level, the main difference was a decrease in the relative abundance of some phylogenetic groups (Fig. 3a), suggesting a sensitivity of those groups to contamination. At the transcriptomic level (Fig. 3b), few taxa appear characteristic of each mat. Only *Parvularculales* within *Alphaproteobacteria* were characteristic taxa of the contaminated mat. *Alphaproteobacteria* are key contributors to the later stages of oil degradation [41]. However, hydrocarbon degradation is strain specific; phylogenetic description based on taxonomic genes such as 16SrRNA (especially when this description is performed at high phylogenetic levels such as the order) has low explanatory value, since two strains belonging to the same taxon can be or not hydrocarbonoclastic. Using short reads approaches, affiliation of sequences below the genus, or even the family, is often unattainable.

The greatest differences in metabolic potential at the metagenomics level were related to signal transduction and membrane transport. These pathways were significantly more abundant in the hydrocarbon-contaminated microbial mat, whereas nucleotide metabolism and replication and repair pathways were significantly more abundant in the reference mat (Fig. 4). The contaminated mat was enriched with genes involved in two component systems (signal transduction, TCS) of the OmpR family (involved in copper ion efflux and manganese transport as a response of Mn starvation) and NtrC family (involved in nitrogen availability) (Table S4). The TCS are known to modify microbial physiology in response to multiple environmental signals and thus playing a role in biogeochemical cycles. Indeed, marine bacteria have varied TCS systems, and it has been proposed that lack of TCS could be a hallmark of oligotrophy in marine systems [42]. Contaminated mat is probably enriched with TCS as an adaptive response to contamination. The overabundance of membrane transport–related genes concerns the ABC transporters and the type IV (T4SS) secretion systems. Recently, Xu et al. [43] described an enrichment in ABC transporters and TCS after dibutyl phthalate contamination in soils. They also observed an acceleration of nitrogen, carbon and sulphate metabolisms and suggested that ABC transporters and TCS were the culprits of this metabolic activation.

The T4SS are found in gram-negative bacteria, and are capable of secreting a wide variety of substances across the bacterial membranes including toxic bacterial effectors that result in cell death of rival bacteria and eukaryote

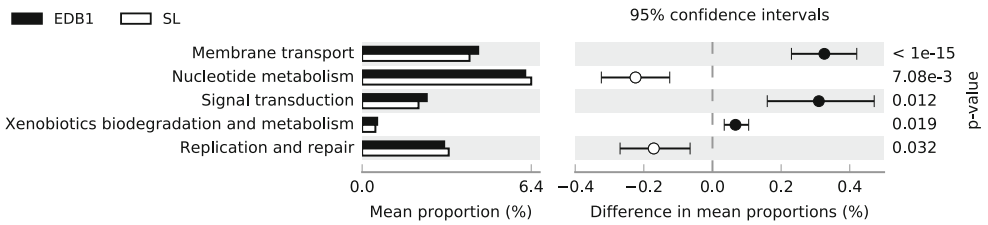

Fig. 4 Comparison (White's non-parametric *t* test in STAMP) of functional gene annotations of metagenomes using KEGG pathways (level 1). Plots compare the hydrocarbon contaminated mat (EDB1) in black to the reference (SL) in white. Only pathways with *p* value below 0.05, with difference in mean proportions above 0.05% are shown

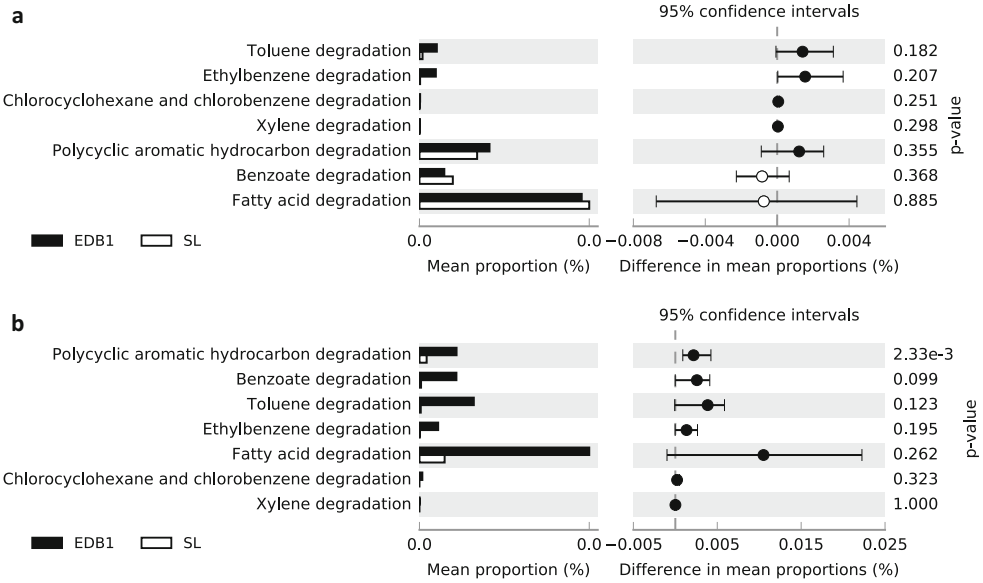

Fig. 5 Extended error plot comparison of the hydrocarbon degradation-related genes or transcripts in the metagenome (**a**) and metatranscriptome (**b**) data. Only the genes involved in the activation of the hydrocarbon molecules were considered (Table S5). The plot compares the hydrocarbon-contaminated mat (EDB1) in black to the reference (SL) in white

[44]. T4SS is ancestrally related to bacterial DNA conjugation systems, and the T4SS-mediated genetic horizontal transfer is considered as a major contributor to bacterial genomic mobility [45]. Altogether, enrichment of ABC transporters and T4SS appears as a mechanism to control the community structure and the metabolic potential in the contaminated microbial mat.

Although less pronounced, xenobiotic biodegradation and metabolism pathways were significantly more abundant in the contaminated mat than in the reference mat. At the metatranscriptomic level, no differences in xenobiotic biodegradation and metabolism nor in the other level1 KEGG metabolic pathways were observed between the two mats (p value > 0.05 or difference in mean proportions $< 0.05\%$).

To further characterize the hydrocarbon degradation potential of the mats, genes involved in hydrocarbon molecule activation were retrieved from the whole dataset (Fig. 5a; Table S5). These genes are specifically associated with hydrocarbon degradation, whereas those involved in intermediate reactions can be shared with other metabolic pathways (http://www.genome.jp/kegg/pathway.html). The gene encoding alkane 1-monooxygenase (*alkB*) (the single representative of genes involved in the fatty acid degradation pathway, Table S5), which is responsible for alkane activation, was more abundant (Wilcoxon test, p value = 0.03125) than the

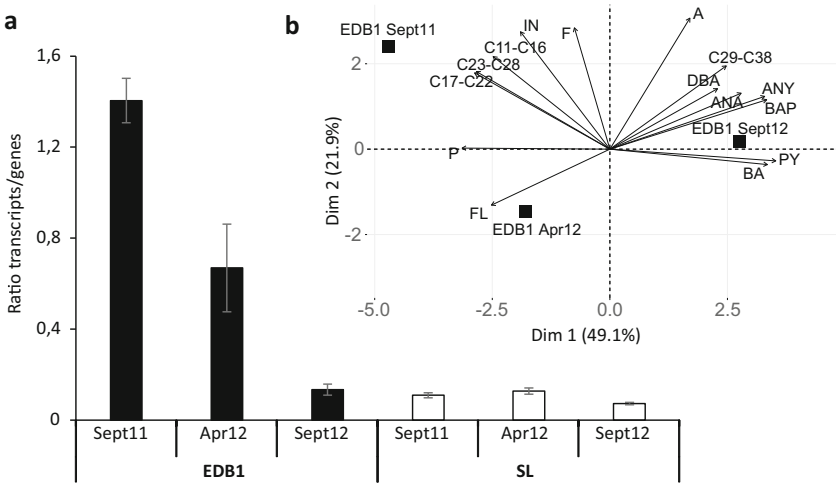

Fig. 6 Expression level of genes involved in hydrocarbon degradation (Table S5) in mats (**a**): in black, contaminated site (EDB1) and in white, reference (SL) mat. Principal component biplot (PCA) based on hydrocarbon contents in EDB1 (**b**). A anthracene, ANA acenaphtene, ANY acenaphtylene, BA benzo(a)anthracene, BAP benzo(a)pyrene, DBA dibenz(a,h)anthracene, F fluorene, FL fluoranthene, IN indeno(1,2,3-cd)pyrene, P phenanthrene, PY pyrene. C11–C16, sum of alkanes from C11 to C16; C17–C22, sum of alkanes from C17 to C23; C24–C28, sum of alkanes from C24 to C28. The parameters with a cos2 below 0.5 are not shown (benzo(g,h,i)perylene; chrysene; naphtalene; benzo(b+k)fluoranthene)

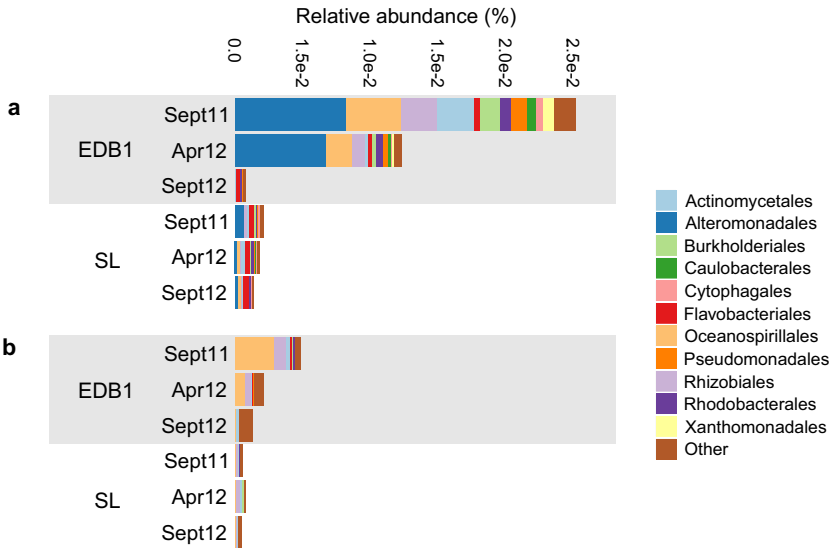

Fig. 7 Relative abundance (%) and affiliation of transcripts involved in the activation of fatty acids (*alkB* transcripts in our study, exclusively) (**a**) and polycyclic aromatic hydrocarbon (**b**) degradation pathways. Figure shows the fraction of reads that hits with the KEGG database. Data represent the mean of the triplicates

genes involved in degradation of aromatic compounds (Fig. 5a), as observed after the Deepwater Horizon oil spill [16]. The relative abundance and taxonomic identification of *alkB* were similar between the contaminated and reference mats (Fig. 5a; Fig. S1). Although the *alkB* gene has been widely used to investigate alkane degradation [46–49] and as a marker of petroleum degradation potential [16], its direct relationship with petroleum hydrocarbon degradation is questionable, especially in chronically contaminated environments [14]. In fact, *alkB* is involved in the degradation of alkanes of both biogenic and petrogenic origin. Biogenic alkanes are the consequence of organic matter degradation and are ubiquitous in nature [50]. As for *alkB*, the relative abundance of all the genes involved in the degradation of aromatic hydrocarbons was similar in both mats (Fig. 5a).

Analysis at the metatranscriptomic level revealed significant higher expression of genes involved in PAH activation in the contaminated mat (Fig. 5b). However, the expression of all the genes involved in HC activation in the contaminated mats decreased over time (Fig. 6a). Interestingly, this decrease was concomitant with changes in hydrocarbon composition during the sampling exercises (Fig. 6b). Short-chain alkanes ($<C_{28}$), medium-weight PAHs and heavy PAHs dominated the hydrocarbons in the first, second and last exercises, respectively. The contaminated mat was therefore enriched in recalcitrant molecules in the last exercise [20], reaching a composition similar to that previously observed at this site [8]. Overall, these results (chemical modification and a decrease in the expression rates of hydrocarbon activation-involved genes) suggest a progressive degradation of the more easily degradable hydrocarbons released by the overflow spill in September 2009.

A decrease in relative abundances was evident for fatty acid degradation activation genes, namely *alkB* (Fig. 7a). The taxonomic affiliations of the *alkB* transcripts suggest *Alteromonadales*-related bacteria as the main alkane degraders in the first sampling exercise, consistent with a previous study of the Berre lagoon in which *Marinobacter aquaeolei* was the dominant *alkB* phylotype [14]. The relative abundance of *alkB* transcripts decreased over time in parallel with the decrease in lower-molecular-weight alkanes. Transcripts involved in PAH degradation also decreased, albeit to a lesser extent, with *Oceanospirillales*-related bacteria as the main actors (Fig. 7b).

Conclusion

Both mats displayed a typical structure and functioning, with dominance of *Cyanobacteria* and sulphur cycle–related microorganisms. Genes involved in environmental information processing were overabundant in the contaminated mat compared with the reference one. However, xenobiotic degradation metabolisms represented a minor part of the metagenome and metatranscriptome, and no overabundance of hydrocarbonoclastic bacteria was observed in the contaminated mat. The expression levels of genes associated with hydrocarbon degradation pathways varied between the mats and among sampling exercises. In the contaminated mat, the expression of genes responsible for hydrocarbon activation was related to hydrocarbon composition, suggesting degradation of easily degradable molecules. The studied mat appeared robust enough to cope with hydrocarbon contamination but its seasonal behaviour was affected.

Acknowledgments The authors received support with linguistic proofreading from a professional proofreading service.

Funding Information This work was supported by the French National Research Agency (ANR FUNHYMAT ANR11 BSV7 014 01).

References

1. Allen MA, Goh F, Burns BP, Neilan BA (2009) Bacterial, archaeal and eukaryotic diversity of smooth and pustular microbial mat communities in the hypersaline lagoon of Shark Bay. Geobiology 7:82–96. https://doi.org/10.1111/j.1472-4669.2008.00187.x
2. van Gemerden H (1993) Microbial mats: a joint venture. Mar Geol 113:3–25
3. Vincent WF (2002) Cyanobacterial dominance in the polar regions. In: Whitton BA, Potts M (eds) The Ecology of Cyanobacteria. Springer, Netherlands, pp 321–340
4. Dillon JG, Miller S, Bebout B, Hullar M, Pinel N, Stahl DA (2009) Spatial and temporal variability in a stratified hypersaline microbial mat community. FEMS Microbiol Ecol 68:46–58. https://doi.org/10.1111/j.1574-6941.2009.00647.x
5. Harris JK, Caporaso JG, Walker JJ, Spear JR, Gold NJ, Robertson CE, Hugenholtz P, Goodrich J, McDonald D, Knights D, Marshall P, Tufo H, Knight R, Pace NR (2013) Phylogenetic stratigraphy in the Guerrero Negro hypersaline microbial mat. ISME J 7:50–60. https://doi.org/10.1038/ismej.2012.79
6. Schneider D, Arp G, Reimer A, Reitner J, Daniel R (2013) Phylogenetic analysis of a microbialite-forming microbial mat from a hypersaline lake of the Kiritimati Atoll, Central Pacific. PLoS One 8:e66662. https://doi.org/10.1371/journal.pone.0066662
7. Barth HJ (2003) The influence of cyanobacteria on oil polluted intertidal soils at the Saudi Arabian Gulf shores. Mar Pollut Bull 46:1245–1252. https://doi.org/10.1016/S0025-326X(03)00374-6
8. Paissé S, Coulon F, Goñi-Urriza M, Peperzak L, McGenity T, Duran R (2008) Structure of bacterial communities along a hydrocarbon contamination gradient in a coastal sediment. FEMS Microbiol Ecol 66:295–305. https://doi.org/10.1111/j.1574-6941.2008.00589.x
9. Bordenave S, Goñi-Urriza MS, Caumette P, Duran R (2007) Effects of heavy fuel oil on the bacterial community structure of a pristine microbial mat. Appl Environ Microbiol 73:6089–6097. https://doi.org/10.1128/AEM.01352-07
10. Paissé S, Goñi-Urriza M, Stadler T et al (2012) Ring-hydroxylating dioxygenase (RHD) expression in a microbial community during the early response to oil pollution. FEMS Microbiol Ecol 80:77–86. https://doi.org/10.1111/j.1574-6941.2011.01270.x
11. Abed RMM, Safi NMD, Köster J, de Beer D, el-Nahhal Y, Rullkötter J, Garcia-Pichel F (2002) Microbial diversity of a heavily polluted microbial mat and its community changes following degradation of petroleum compounds. Appl Environ Microbiol 68:1674–1683. https://doi.org/10.1128/AEM.68.4.1674-1683.2002
12. Paisse S, Goni-Urriza M, Coulon F, Duran R (2010) How a bacterial community originating from a contaminated coastal sediment responds to an oil input. Microb Ecol 60:394–405. https://doi.org/10.1007/s00248-010-9721-7
13. Abed RMM, Al-Kharusi S, Prigent S, Headley T (2014) Diversity, distribution and hydrocarbon biodegradation capabilities of microbial communities in oil-contaminated cyanobacterial mats from a constructed wetland. PLoS One 9:e114570. https://doi.org/10.1371/journal.pone.0114570
14. Paisse S, Duran R, Coulon F, Goñi-Urriza M (2011) Are alkane hydroxylase genes (alkB) relevant to assess petroleum bioremediation processes in chronically polluted coastal sediments? Appl Microbiol Biotechnol 92:835–844. https://doi.org/10.1007/s00253-011-3381-5
15. Lu Z, Deng Y, Van Nostrand JD et al (2012) Microbial gene functions enriched in the Deepwater Horizon deep-sea oil plume. ISME J 6:451–460. https://doi.org/10.1038/ismej.2011.91
16. Mason OU, Hazen TC, Borglin S, Chain PS, Dubinsky EA, Fortney JL, Han J, Holman HY, Hultman J, Lamendella R, Mackelprang R, Malfatti S, Tom LM, Tringe SG, Woyke T, Zhou J, Rubin EM, Jansson JK (2012) Metagenome, metatranscriptome and single-cell sequencing reveal microbial response to Deepwater Horizon oil spill. Isme J 6:1715–1727. https://doi.org/10.1038/ismej.2012.59
17. Rivers AR, Sharma S, Tringe SG, Martin J, Joye SB, Moran MA (2013) Transcriptional response of bathypelagic marine bacterioplankton to the Deepwater Horizon oil spill. ISME J 7:2315–2329. https://doi.org/10.1038/ismej.2013.129
18. de Menezes A, Clipson N, Doyle E (2012) Comparative metatranscriptomics reveals widespread community responses during phenanthrene degradation in soil. Environ Microbiol 14:2577–2588. https://doi.org/10.1111/j.1462-2920.2012.02781.x
19. Mason OU, Scott NM, Gonzalez A, Robbins-Pianka A, Bælum J, Kimbrel J, Bouskill NJ, Prestat E, Borglin S, Joyner DC, Fortney JL, Jurelevicius D, Stringfellow WT, Alvarez-Cohen L, Hazen TC, Knight R, Gilbert JA, Jansson JK (2014) Metagenomics reveals sediment microbial community response to Deepwater Horizon oil spill. ISME J 8:1464–1475. https://doi.org/10.1038/ismej.2013.254
20. Aubé J, Senin P, Pringault O, Bonin P, Deflandre B, Bouchez O, Bru N, Biritxinaga-Etchart E, Klopp C, Guyoneaud R, Goñi-Urriza M (2016) The impact of long-term hydrocarbon exposure on the structure, activity, and biogeochemical functioning of microbial mats. Mar Pollut Bull 111:115–125. https://doi.org/10.1016/j.marpolbul.2016.07.023
21. Pringault O, Aube J, Bouchez O et al (2015) Contrasted effects of natural complex mixtures of PAHs and metals on oxygen cycle in a microbial mat. Chemosphere 135:189–201. https://doi.org/10.1016/j.chemosphere.2015.04.037
22. Beau-Monvoisin N (2009) Déversement accidentel d'hydrocarbures, sur l'étang de Berre suite à un débordement des bassins d'orage de la Compagnie Pétrochimique de Berre (CPB). Brest : Cedre (Centre de documentation de recherche et d'expérimentations sur les pollutions accidentelles des eaux)
23. Martin M (2011) Cutadapt removes adapter sequences from high-throughput sequencing reads. EMBnet.journal 17:10–12. https://doi.org/10.14806/ej.17.1.200
24. Kanehisa M, Goto S (2000) KEGG: Kyoto Encyclopedia of Genes and Genomes. Nucleic Acids Res 28:27–30
25. Frith MC, Hamada M, Horton P (2010) Parameters for accurate genome alignment. BMC Bioinformatics 11:80. https://doi.org/10.1186/1471-2105-11-80
26. Moriya Y, Itoh M, Okuda S, Yoshizawa AC, Kanehisa M (2007) KAAS: an automatic genome annotation and pathway reconstruction server. Nucleic Acids Res 35:W182–W185. https://doi.org/10.1093/nar/gkm321
27. Segata N, Waldron L, Ballarini A, Narasimhan V, Jousson O, Huttenhower C (2012) Metagenomic microbial community profiling using unique clade-specific marker genes. Nat Methods 9:811–814. https://doi.org/10.1038/nmeth.2066
28. Parks DH, Tyson GW, Hugenholtz P, Beiko RG (2014) STAMP: statistical analysis of taxonomic and functional profiles. Bioinformatics 30:3123–3124. https://doi.org/10.1093/bioinformatics/btu494
29. Stewart FJ, Ulloa O, DeLong EF (2012) Microbial metatranscriptomics in a permanent marine oxygen minimum zone. Environ Microbiol 14:23–40. https://doi.org/10.1111/j.1462-2920.2010.02400.x
30. Lê S, Rennes A, Josse J et al (2008) FactoMineR: an R package for multivariate analysis. J Stat Softw:1–18
31. Bolhuis H, Stal LJ (2011) Analysis of bacterial and archaeal diversity in coastal microbial mats using massive parallel 16S rRNA gene tag sequencing. Isme J 5:1701–1712. https://doi.org/10.1038/Ismej.2011.52

32. Severin I, Acinas SG, Stal LJ (2010) Diversity of nitrogen-fixing bacteria in cyanobacterial mats. FEMS Microbiol Ecol 73:514–525. https://doi.org/10.1111/j.1574-6941.2010.00925.x
33. Robertson CE, Spear JR, Harris JK, Pace NR (2009) Diversity and stratification of archaea in a hypersaline microbial mat. Appl Environ Microbiol 75:1801–1810. https://doi.org/10.1128/AEM.01811-08
34. Mobberley JM, Khodadad CLM, Visscher PT, Reid RP, Hagan P, Foster JS (2015) Inner workings of thrombolites: spatial gradients of metabolic activity as revealed by metatranscriptome profiling. Sci Rep 5:12601. https://doi.org/10.1038/srep12601
35. Wieland A, Zopfi J, Benthien M, Kühl M (2005) Biogeochemistry of an iron-rich hypersaline microbial mat (Camargue, France). Microb Ecol 49:34–49. https://doi.org/10.1007/s00248-003-2033-4
36. Pinckney J, Paerl HW, Fitzpatrick M (1996) Impacts of seasonality and nutrients on microbial mat community structure and function. Oceanogr Lit Rev 3:283
37. Lamendella R, Strutt S, Borglin SE, Chakraborty R, Tas N, Mason OU, Hultman J, Prestat E, Hazen TC, Jansson JK (2014) Assessment of the Deepwater Horizon oil spill impact on gulf coast microbial communities. Aquat Microbiol 5:130. https://doi.org/10.3389/fmicb.2014.00130
38. Atlas RM, Stoeckel DM, Faith SA, Minard-Smith A, Thorn JR, Benotti MJ (2015) Oil biodegradation and oil-degrading microbial populations in marsh sediments impacted by oil from the Deepwater Horizon well blowout. Environ Sci Technol 49:8356–8366. https://doi.org/10.1021/acs.est.5b00413
39. Nogales B, Lanfranconi MP, Piña-Villalonga JM, Bosch R (2011) Anthropogenic perturbations in marine microbial communities. FEMS Microbiol Rev 35:275–298. https://doi.org/10.1111/j.1574-6976.2010.00248.x
40. Cappello S, Caruso G, Zampino D, Monticelli LS, Maimone G, Denaro R, Tripodo B, Troussellier M, Yakimov M, Giuliano L (2007) Microbial community dynamics during assays of harbour oil spill bioremediation: a microscale simulation study. J Appl Microbiol 102:184–194. https://doi.org/10.1111/j.1365-2672.2006.03071.x
41. Kostka JE, Prakash O, Overholt WA, Green SJ, Freyer G, Canion A, Delgardio J, Norton N, Hazen TC, Huettel M (2011) Hydrocarbon-degrading bacteria and the bacterial community response in Gulf of Mexico beach sands impacted by the Deepwater horizon oil spill. Appl Environ Microbiol 77:7962–7974. https://doi.org/10.1128/AEM.05402-11
42. Held NA, McIlvin MR, Moran DM et al (2019) Unique patterns and biogeochemical relevance of two-component sensing in marine bacteria. mSystems 4:e00317–e00318. https://doi.org/10.1128/mSystems.00317-18
43. Xu W, You Y, Wang Z, Chen W, Zeng J, Zhao X, Su Y (2018) Dibutyl phthalate alters the metabolic pathways of microbes in black soils. Sci Rep 8:2605. https://doi.org/10.1038/s41598-018-21030-8
44. Green ER, Mecsas J (2016) Bacterial secretion systems: an overview. Microbiol Spectr 4. https://doi.org/10.1128/microbiolspec.VMBF-0012-2015
45. Waksman G (2019) From conjugation to T4S systems in gram-negative bacteria: a mechanistic biology perspective. EMBO Rep 20:e47012. https://doi.org/10.15252/embr.201847012
46. Vomberg A, Klinner U (2000) Distribution of alkB genes within n-alkane-degrading bacteria. J Appl Microbiol 89:339–348. https://doi.org/10.1046/j.1365-2672.2000.01121.x
47. Van Beilen JB, Li Z, Duetz WA et al (2003) Diversity of alkane hydroxylase systems in the environment. Oil Gas Sci Technol 58:427–440. https://doi.org/10.2516/ogst:2003026
48. van Beilen JB, Funhoff EG (2007) Alkane hydroxylases involved in microbial alkane degradation. Appl Microbiol Biotechnol 74:13–21. https://doi.org/10.1007/s00253-006-0748-0
49. Smith CB, Tolar BB, Hollibaugh JT, King GM (2013) Alkane hydroxylase gene (alkB) phylotype composition and diversity in northern Gulf of Mexico bacterioplankton. Front Microbiol 4. https://doi.org/10.3389/fmicb.2013.00370
50. Widdel F, Rabus R (2001) Anaerobic biodegradation of saturated and aromatic hydrocarbons. Curr Opin Biotechnol 12:259–276. https://doi.org/10.1016/S0958-1669(00)00209-3